

Fabry-Perot complex plasmonic eigenfrequencies for equally spaced noble-metal parallel plates

Jamal T. Manassah*

Department of Electrical Engineering, City College of New York, New York, New York 10031, USA

(Received 23 July 2012; published 1 November 2012)

The eigenvalue condition for computing the Fabry-Perot eigenmodes of n -identical equally spaced metallic parallel plates is obtained. The frequency and decay rate of the plasmonic resonances for gold and silver are computed for quarter-wave metallic plates. I show that the system's plasmonic frequency can be tuned in silver to any desired value in the optical regime through a specific choice of the ratio of the dielectric to metal plate thickness. I also show that the eigenmodes with wave vectors having $\text{Re}(v) \cong 0$ form narrow resonances.

DOI: [10.1103/PhysRevA.86.053801](https://doi.org/10.1103/PhysRevA.86.053801)

PACS number(s): 42.70.Qs, 78.67.Pt

I. INTRODUCTION

As far back as the end of the 19th century, Lord Rayleigh [1] studied the propagation of waves in periodically stratified media. This field has remained an active area of research since then. The advances made in this field until the 1950's are summarized in the classic book of Brillouin [2], who himself made seminal contributions to the advancement of this field. A landmark in modern physics is the work of Bloch [3], who generalized the work of Floquet [4] on the solutions of differential equations with a periodic potential to lay the foundations for the theory of electrons in crystals. In optics, the field was pioneered by Abeles [5], who formulated an elegant approach for treating problems of stratified optical thin films. This formulation was at the basis of the later theoretical treatment of filters, antireflection films, beam splitters, and polarizers. In the past four decades, the theory of periodic structures provided as well the framework for the development of theories of distributed feedback lasers [6,7] and photonic crystals [8]. Friedberg and I [9] benefited from all these earlier works to analyze the phenomenon of "precocious superradiance" earlier predicted by myself [10].

Recently, finding the resonant plasmonic frequencies of different geometric structures became highly sought in the exploding field of nanoscience. Different approaches for finding the resonant plasmonic frequencies for different geometric structures used tools from perturbatively corrected electrostatics [11], the hybridization theory of quantum chemistry [12], and the theory of electrodynamics eigenfunctions [13]. In this paper, I use the theory of transfer matrices earlier reformulated in Ref. [9] to find the plasmonic complex eigenfrequencies of a stack of parallel quarter plates of noble metals (silver and gold) alternating with plates of a dielectric. This configuration is of interest at both the microscopic and nanoscopic levels. (Results from experiments on an ensemble of nanospheres interacting with a metallic planar structure already have been reported on in the literature [14].)

The objective of this paper is to obtain the Fabry-Perot complex eigenfrequencies of the system when the periodic structure has a finite number of elements, when the thickness of the metal plate is a quarter plate of the plasmonic resonance frequency, but that of the dielectric plate is allowed to vary. In particular, the ratio of the thickness of the dielectric to metal

plate thickness is identified as the parameter which controls the tuning of the plasmonic resonant frequency. The eigenmodes of the system which have small decay rates are identified as well. The mode with a near-zero value for the real part of its wave vector is found in all cases to be the best candidate. Both results help achieve the stated goal of facilitating the identification of the narrow plasmonic resonances of the system.

In Sec. II, the mathematical tools [9] that will subsequently be used in the calculations are reviewed. In Sec. III, the transfer matrix for a unit cell ($\frac{1}{2}$ dielectric plate, 1 metal plate, $\frac{1}{2}$ dielectric plate) is derived. In Sec. IV, the eigenvalue condition for the combined system is calculated. In Sec. V, the expression and parameters of the Drude model used in the constitutive equation (dielectric function as function of the frequency) for the metal are given. In Sec. VI, the complex eigenfrequencies of interest are computed. Section VII concludes.

II. MATHEMATICAL BACKGROUND

In this section, I shall review, in the language of transfer matrices, the mathematical techniques that I use in obtaining the eigenmodes of an arbitrary system consisting of multislices, and as previously derived in Ref. [9].

In the present geometry, I shall consider the propagation normal to the plates, and therefore only the Fabry-Perot modes (and not the waveguiding modes) shall be considered. Furthermore, the electric field shall be taken to be a scalar. [The transverse electric (TE) and transverse magnetic (TM) modes are indistinguishable.]

I shall first give the elementary transfer matrices from which all subsequent ones for the multislice problems can be constructed. Then I summarize other theorems that will prove useful in obtaining or verifying subsequently reported results.

In one-dimensional (1D) structures, the classical field to the left of $z \cong z_L$ in the same uniform medium can be written as

$$\Phi_L(z) = A_L \exp[-ik_L(z - z_L)] + B_L \exp[ik_L(z - z_L)]. \quad (1)$$

Similarly, the classical field to the right of $z \cong z_R$ in the same medium can be written as

$$\Phi_R(z) = A_R \exp[-ik_R(z - z_R)] + B_R \exp[ik_R(z - z_R)]. \quad (2)$$

*jmanassah@gmail.com

The transfer matrix \mathbf{M} is defined as

$$\begin{pmatrix} A_L \\ B_L \end{pmatrix} = \mathbf{M} \begin{pmatrix} A_R \\ B_R \end{pmatrix}. \quad (3)$$

Theorem 1: The interface transfer matrix between two regions is equal to

$$\begin{aligned} \mathbf{M} &= \mathbf{M}^{\mathbf{B}}(k_L, k_R) = \frac{1}{2k_L} \begin{pmatrix} k_L + k_R & k_L - k_R \\ k_L - k_R & k_L + k_R \end{pmatrix} \\ &= \frac{1}{2k_L} [(k_L + k_R)\mathbf{I} + (k_L - k_R)\tau_1] \\ &= \exp[\lambda(\tau_1 - \mathbf{I})], \end{aligned} \quad (4)$$

where $\lambda = \frac{1}{2} \ln(\frac{k_L}{k_R})$, \mathbf{I} is the $(2 \otimes 2)$ identity matrix, and τ 's are the Pauli matrices given by

$$\tau_1 = \begin{pmatrix} 0 & 1 \\ 1 & 0 \end{pmatrix}, \quad \tau_2 = \begin{pmatrix} 0 & -i \\ i & 0 \end{pmatrix}, \quad \tau_3 = \begin{pmatrix} 1 & 0 \\ 0 & -1 \end{pmatrix}. \quad (5)$$

Proof: At the interface between two media, we have $z = z_L = z_R$. At that point, the field and its derivative should be continuous ($\Phi_L = \Phi_R$ and $\frac{d\Phi_L}{dz} = \frac{d\Phi_R}{dz}$). These boundary conditions lead to the system of equations:

$$A_L + B_L = A_R + B_R, \quad (6a)$$

$$k_L(A_L - B_L) = k_R(A_R - B_R). \quad (6b)$$

This system of equations represents the first equality in Eq. (4).

Then, we used the Pauli's algebra result that

$$\exp(i\vec{\tau} \cdot \hat{\mathbf{n}}\theta) = \cos(\theta)\mathbf{I} + i\vec{\tau} \cdot \hat{\mathbf{n}} \sin(\theta) \quad (7)$$

in going from the first line to the second line of Eq. (4).

Theorem 2: The transfer matrix representing the propagation in a uniform medium is given by

$$\mathbf{M} = \mathbf{M}^{\mathbf{P}}(kl) = \begin{pmatrix} \exp(ikl) & 0 \\ 0 & \exp(-ikl) \end{pmatrix} = \exp(ikl\tau_3), \quad (8)$$

where l is the distance of propagation.

Proof: In propagating in a uniform medium, only the field phase changes. If $k_L = k_R = k$ and $z_R - z_L = l$, then

$$A_L \exp(ikz_L) = A_R \exp(ikz_R), \quad (9a)$$

$$B_L \exp(-ikz_L) = B_R \exp(-ikz_R). \quad (9b)$$

Combining Eqs. (9) and (7), one obtains Eq. (8).

Theorem 3 (Invisible gap theorem): Inserting a gap with $kl = m\pi$ (where l is the length of the gap and k is the wave vector of propagation in the gap) at any location within a uniform medium will at most change the sign of the overall transfer matrix.

Proof: Let the wave vector in the uniform medium where the insertion occurs be denoted by k' . Then the transfer matrix corresponding to this insertion is given by

$$\begin{aligned} \mathbf{M}^{\text{gap}}(k', kL, k') &= \mathbf{M}^{\mathbf{B}}(k', k)\mathbf{M}^{\mathbf{P}}(kL)\mathbf{M}^{\mathbf{B}}(k, k') \\ &= \exp[\lambda(\mathbf{I} - \tau_1)] \exp(ikL\tau_3) \exp[-\lambda(\mathbf{I} - \tau_1)] \\ &= \exp[\lambda(\mathbf{I} - \tau_1)] [\cos(kL)\mathbf{I} + i \sin(kL)\tau_3] \\ &\quad \times \exp[-\lambda(\mathbf{I} - \tau_1)], \end{aligned} \quad (10)$$

where $\lambda = \frac{1}{2} \ln(\frac{k'}{k})$. We used Eq. (7) to go from the second to third line in Eq. (10).

If $kL = m\pi$, the square bracket in Eq. (10) reduces to $(-1)^m \mathbf{I}$, consequently giving

$$\mathbf{M}^{\text{gap}}(k', kL = m\pi, k') = (-1)^m \mathbf{I}. \quad (11)$$

Theorem 4: The eigenmodes of a system are obtained by solving the equation

$$(\mathbf{M}^{\mathbf{T}})_{22} = 0. \quad (12)$$

Proof: The eigenmode condition is obtained by noting that, in that instance, only outgoing fields should exist on the left- and right-hand sides of the total transfer matrix of the system, i.e., $B_L = A_R = 0$.

The above constraint leads to the identity $0 = (\mathbf{M}^{\mathbf{T}})_{22} B_R$, which requires that $(\mathbf{M}^{\mathbf{T}})_{22} = 0$.

Theorem 5 (The Cayley-Hamilton-Sylvester theorem): This theorem gives a closed-form expression for the n th power of a unimodular matrix (a matrix whose determinant is equal to 1).

For the unimodular matrix given by

$$\mathbf{M} = \begin{pmatrix} a & b \\ c & d \end{pmatrix}, \quad (13)$$

its n th power is given by

$$\mathbf{M}^n = \begin{pmatrix} \frac{a \sin(n\theta) - \sin[(n-1)\theta]}{\sin(\theta)} & \frac{b \sin(n\theta)}{\sin(\theta)} \\ \frac{c \sin(n\theta)}{\sin(\theta)} & \frac{d \sin(n\theta) - \sin[(n-1)\theta]}{\sin(\theta)} \end{pmatrix}, \quad (14)$$

where

$$\cos(\theta) = \frac{1}{2}(a + d). \quad (15)$$

Proof: As the matrix \mathbf{M} is unimodular, its eigenvalues can be written in the simple form $\lambda_{1,2} = \exp(\pm i\theta)$ to ensure that the value of the determinant is 1. Equation (15) is directly obtained from the invariance of the trace, upon a unitary transformation.

As \mathbf{M} is a $(2 \otimes 2)$ matrix, using the Cayley-Hamilton theorem, one can write its n th power in the form

$$\mathbf{M}^n = \delta \mathbf{I} + \mu \mathbf{M}. \quad (16)$$

Using again the Cayley-Hamilton theorem, which states that a matrix obeys the same equations as its eigenvalues, we deduce that

$$\exp(in\theta) = \delta + \mu \exp(i\theta), \quad (17a)$$

$$\exp(-in\theta) = \delta + \mu \exp(-i\theta). \quad (17b)$$

The system (17) of two equations in two unknowns can be solved to give

$$\mu = \frac{\sin(n\theta)}{\sin(\theta)}, \quad (18a)$$

$$\delta = -\frac{\sin[(n-1)\theta]}{\sin(\theta)}, \quad (18b)$$

from which one obtains directly Eq. (14), which constitutes the statement of the Sylvester theorem.

III. TRANSFER MATRIX FOR THE UNIT CELL

Consider the unit cell consisting of the following structure:

$$\begin{aligned} 0 \leq z \leq \beta l/2 & \text{ dielectric,} \\ \beta l/2 \leq z \leq \beta l/2 + l & \text{ metal,} \\ \beta l/2 + l \leq z \leq \beta l + l & \text{ dielectric,} \end{aligned}$$

and vacuum everywhere else.

The matrix \mathbf{M}^C corresponding to this unit cell is given by

$$\mathbf{M}^C = \mathbf{M}^P(\beta kl/2) \mathbf{M}^B(k, k') \mathbf{M}^P(k') \mathbf{M}^B(k', k) \mathbf{M}^P(\beta kl/2), \quad (19)$$

where k and k' are, respectively, the wave numbers in the dielectric and in the metal.

Introducing the dimensionless variables $u = kl$, $v = k'l$, and $\lambda = \frac{1}{2} \ln(\frac{u}{v})$, the matrix \mathbf{M}^C can be expressed as

$$\begin{aligned} \mathbf{M}^C = & [\cos(\beta u) \cos(v) - \sin(\beta u) \cosh(2\lambda) \sin(v)] \mathbf{I} \\ & + i[\sin(\beta u) \cos(v) + \cos(\beta u) \cosh(2\lambda) \sin(v)] \tau_3 \\ & + \sinh(2\lambda) \sin(v) \tau_2. \end{aligned} \quad (20)$$

IV. EIGENVALUE CONDITION FOR A SYSTEM WITH n CELLS

Let us next compute the transfer matrix for a system consisting of n unit cells placed in series. Its general expression is given by

$$\mathbf{M}^T = \mathbf{M}^B(u_0, u) (\mathbf{M}^C)^n \mathbf{M}^B(u, u_0), \quad (21)$$

where $u = n_r u_0$ and n_r is the index of refraction of the dielectric material.

From Theorem 5 and Eq. (20), one obtains

$$\cos(\theta) = \cos(\beta u) \cos(v) - \sin(\beta u) \cosh(2\lambda) \sin(v), \quad (22)$$

where $\lambda = \frac{1}{2} \ln(\frac{u}{v})$.

The eigenvalue condition $\mathbf{M}_{22}^T = 0$, with \mathbf{M}_{22}^T given by Eqs. (20) and (21) and θ given by Eq. (22), shall be used to compute numerically complex v for each of the modes.

For $n_r = 1$, the eigenvalue condition can be written in the simple form

$$\begin{aligned} & [\sin(\beta u_0) \cos(v) + \cos(\beta u_0) \cosh(2\lambda) \sin(v)] \\ & = -i \sin(\theta) \cot(n\theta). \end{aligned} \quad (23)$$

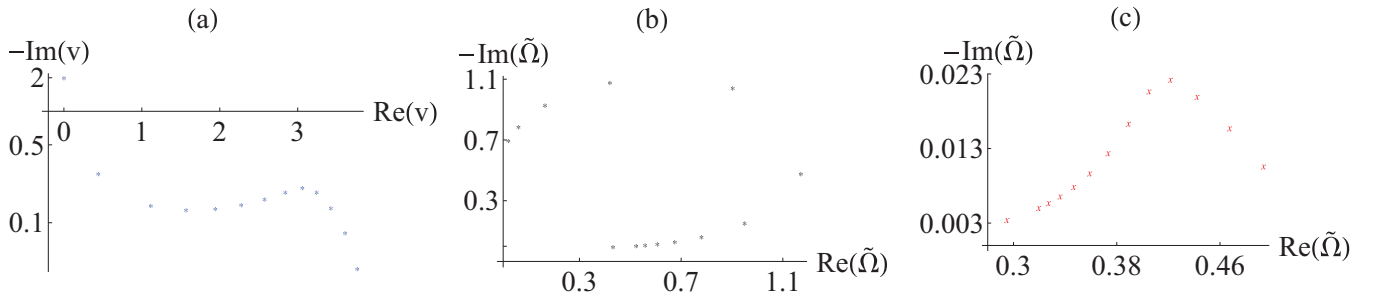


FIG. 1. (Color online) Quantities shown are for all modes with $\text{Re}(v) < 4$. The ratio of the dielectric to metal plate thickness, $\beta = 1$. The number of cells, $n = 10$. (a) The locus of the normalized complex wave vectors. (b) The locus of the normalized complex eigenfrequencies. Silver [the origin of the axes in this graph is at $(0, -0.1)$]. (c) The locus of the normalized complex eigenfrequencies. Gold.

V. THE DIELECTRIC FUNCTION FOR THE METAL

Having obtained the complex wave number of a mode, by finding a solution of the system of equations (22) and $\mathbf{M}_{22}^T = 0$, the plasmonic resonance frequency and the decay rate of the mode are directly obtained by using the frequency-dependent dielectric function of the metal, which we assume here to be given by the Drude model,

$$\varepsilon(\omega) = \varepsilon_\infty - \frac{\omega_p^2}{\omega^2 + i\gamma\omega}, \quad (24)$$

and the dispersion relation

$$\varepsilon(\omega^{(s)}) = \frac{v_s^2}{u_0^2}. \quad (25)$$

We shall further assume the validity of the Kramer-Kronig relations (which only requires causality) and analytically continue (24) in the lower complex plane. The normalized complex eigenfrequency can be written

$$\tilde{\Omega}^{(s)} = \frac{\tilde{\omega}^{(s)}}{\omega_p} = \frac{1}{2} \left(-i\Gamma + \sqrt{\frac{4}{\varepsilon_\infty - \frac{v_s^2}{u_0^2}} - \Gamma^2} \right), \quad (26)$$

where $\Gamma = \gamma/\omega_p$ and s is the index of the mode. $\text{Re}(\tilde{\Omega}^{(s)})$ is the plasmonic resonance frequency of the mode s and $-\text{Im}(\tilde{\Omega}^{(s)})$ is its decay rate.

In the subsequent numerical computations I shall use the Drude's parameters for silver and gold as fitted by Sonnichsen [15] from Johnson and Christy's data [16], namely,

$$\begin{aligned} \text{Ag} : \varepsilon_\infty = 3.7, \quad \lambda_p = 1.36 \text{ nm}, \quad \Gamma = \gamma/\omega_p = 1.92 \times 10^{-3}, \\ \text{Au} : \varepsilon_\infty = 9.84, \quad \lambda_p = 1.36 \text{ nm}, \quad \Gamma = \gamma/\omega_p = 6.94 \times 10^{-3}. \end{aligned}$$

VI. RESULTS

Let us recall that everywhere in the subsequent results, $u_0 = \pi/2$ (all the metal slabs are quarter-wave plates).

A. Locus of narrow resonances

The functional form of Eq. (26) restricts all narrow resonances to eigenmodes with $\text{Re}(v)/u_0 < \sqrt{\varepsilon_{\text{inf}}}$. Consequently, in my search, I shall consider the set of modes with $\text{Re}(v) < 4$ and thus ensure that I have included all viable candidates.

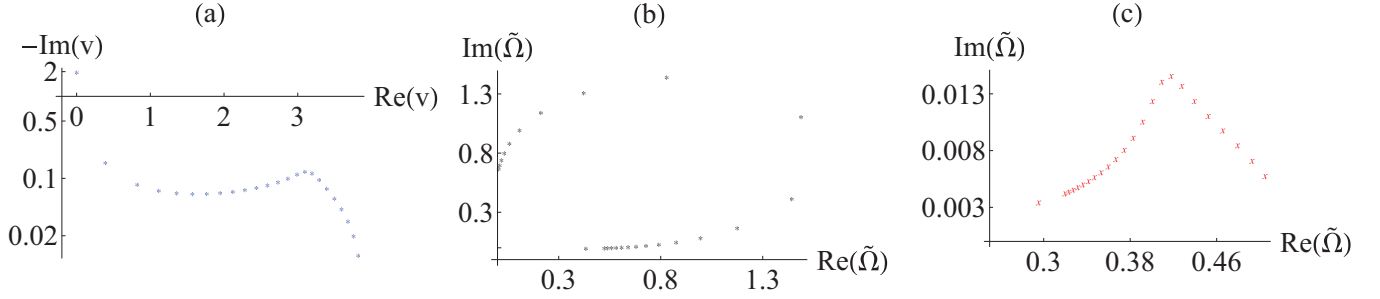


FIG. 2. (Color online) Same as in Fig. 1, except $n = 20$.

The dimension of the ensemble of possible candidates increases with an increase in the number of unit cells. I shall explore the cases where n is large but not excessively so. I shall consider for illustrative purposes the cases of $n = 10$, $n = 20$, and $n = 30$ for $\beta = 1$, $n_r = 1$. I plot in Figs 1–3 the locus of the complex wave vectors and the complex eigenfrequencies for both silver and gold for the above different values of n . It is clear from these figures that not all modes satisfy the narrow mode criterion $[-\text{Im}(\tilde{\Omega}) \approx \Gamma/2]$. Actually, only one such mode strictly satisfies this criterion for $n = 30$, the mode having $\text{Re}(v) \cong 0$.

B. The mode with $\text{Re}(v) \cong 0$

Having established that the decay rate for the mode with $\text{Re}(v) \cong 0$ is comparable to $\Gamma/2$, I explore in Fig. 4 a mechanism for tuning the resonance frequency of this mode. I plot as a function of β the complex wave vector in the metal and the complex eigenfrequency for silver and gold for $n = 20$, for the cases where $n_r = 1$ and $n_r = 3/2$. One notes that it is possible to tune the resonant frequency to any value in the entire optical and near-infrared window by varying the value of β in this structure with silver as the metal. One further notices that the decay rate of this mode approximately maintains its minimum value for all values of β .

In Fig. 5, I explore the dependence of the complex wave vector in the metal and the complex eigenfrequency in silver and gold for different values of β as a function of n , the number of cells. One notes that as n increases beyond 10, almost no change is observed in the different values, leading us to conclude that this mode is very stable.

C. The mode with $\text{Re}(v) \cong \pi/2$

Although I convincingly established above that the mode with $\text{Re}(v) \cong 0$ is the best candidate for the purpose of achiev-

ing tuning to any desired plasmonic frequency resonance, one may still inquire about the variation to the resonance frequency and its decay rate for the other modes as n , the number of unit cells, increases. I choose for this investigation the configuration with $\beta = 1$, and the mode with $\text{Re}(v) \cong \pi/2$ (i.e., the Bragg configuration).

For this mode, I write the wave vector in the form

$$v = \frac{\pi}{2} - i \frac{\Delta}{n}. \tag{27}$$

The expressions for θ and for the eigenvalue condition reduce in this case to

$$\cos(\theta) = -\cosh(2\lambda) \cosh\left(\frac{\Delta}{n}\right), \tag{28}$$

$$\sinh\left(\frac{\Delta}{n}\right) = -\sin(\theta) \cot(n\theta). \tag{29}$$

The next step is to evaluate analytically the different parameters. Making a $(\frac{1}{n})$ expansion, one obtains

$$\cosh(2\lambda) \cong 1 - \frac{2\Delta^2}{n^2\pi^2} - i \frac{4\Delta^3}{n^3\pi^3} + O\left(\left(\frac{1}{n}\right)^4\right), \tag{30}$$

$$\cosh\left(\frac{\Delta}{n}\right) \cong 1 + \frac{\Delta^2}{2n^2} + O\left(\left(\frac{1}{n}\right)^3\right). \tag{31}$$

Inserting Eqs. (30) and (31) in Eq. (28), one obtains

$$\cos(\theta) = -\left(1 + x^2 \frac{\Delta^2}{2n^2}\right), \tag{32}$$

which gives

$$\theta = \pi - i \frac{\Delta}{n} x, \tag{33}$$

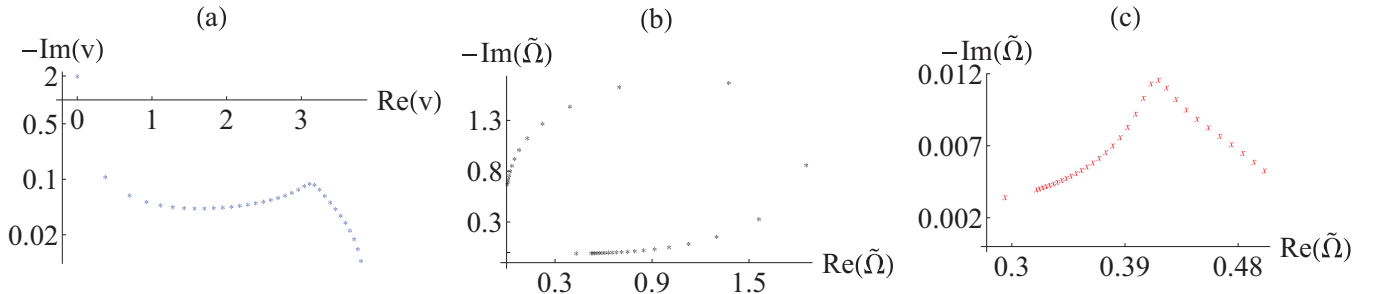


FIG. 3. (Color online) Same as in Fig. 1, except $n = 30$.

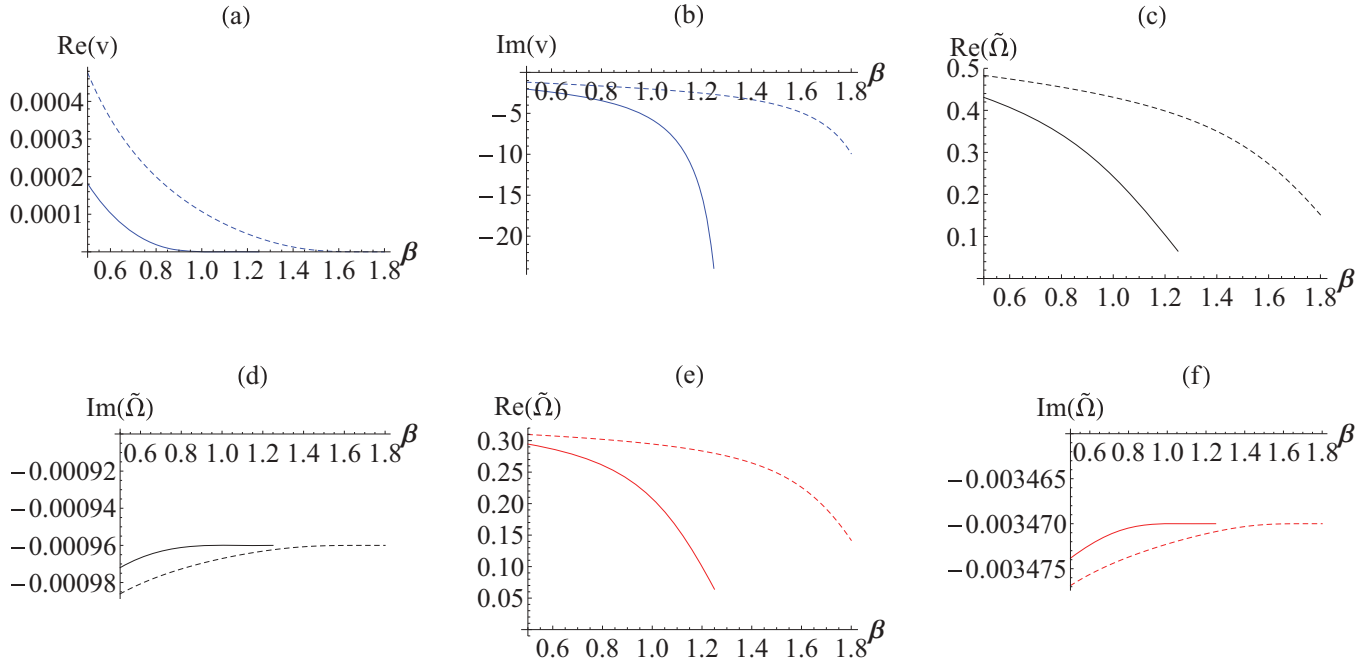


FIG. 4. (Color online) The quantities for the mode with $\text{Re}(v) \cong 0$ are plotted as a function of β , the ratio of the dielectric to metal plate thickness. The number of cells is $n = 20$. Solid line: $n_r = 1.5$. Dashed line: $n_r = 1.0$. (a), (b) The normalized real and imaginary parts of the normalized wave vector. (c), (d) The normalized real and imaginary parts of the plasmonic resonance frequency with silver as the metal. (e), (f) The normalized real and imaginary parts of the plasmonic resonance frequency with gold as the metal.

where

$$\frac{\Delta}{n}x = \left[\frac{\Delta^2}{n^2} - \left(\frac{2}{\pi}\right)^2 \frac{\Delta^2}{n^2} - i \left(\frac{2}{\pi}\right)^3 \frac{\Delta^3}{n^3} \right]^{1/2} \cong \frac{\Delta}{n} \left\{ \left[1 - \left(\frac{2}{\pi}\right)^2 \right]^{1/2} - \frac{i}{n} \left(\frac{4\Delta}{\pi^3 \sqrt{1 - \left(\frac{2}{\pi}\right)^2}} \right) \right\}. \quad (34)$$

Combining (29), (33), and (34), one obtains

$$x \cot(n\theta) = i. \quad (35)$$

Upon a Taylor expansion of $\tanh(x)$ near $x_0 = [1 - (\frac{2}{\pi})^2]^{1/2}$, and using (35), one deduces that

$$\Delta = \Delta_0 - i \frac{\delta}{n}, \quad (36)$$

where $\Delta_0 = 1.327$ and $\delta = 0.328$.

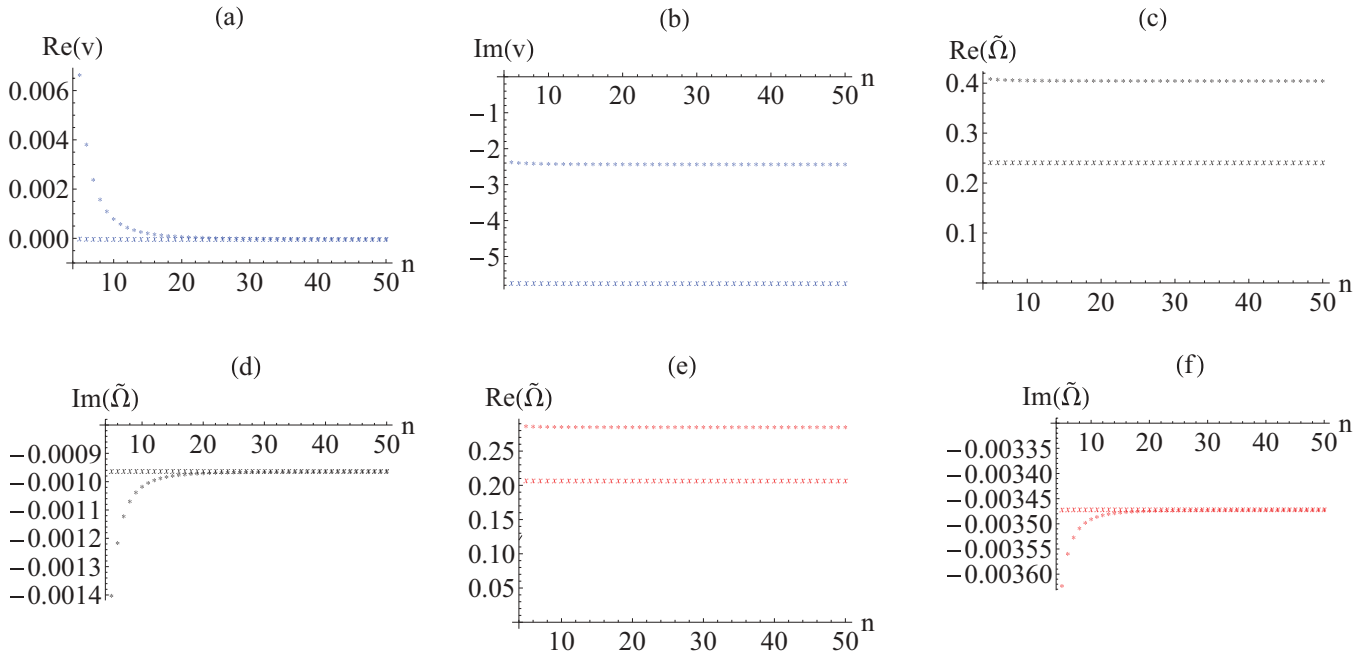


FIG. 5. (Color online) The quantities for the mode with $\text{Re}(v) \cong 0$ are plotted as a function of n , the number of cells. The index of refraction of the dielectric is $n_r = 1.5$. *: $\beta = 0.6$. \times : $\beta = 1$. (a)–(f) are the same quantities as in the graphs of Fig. 4.

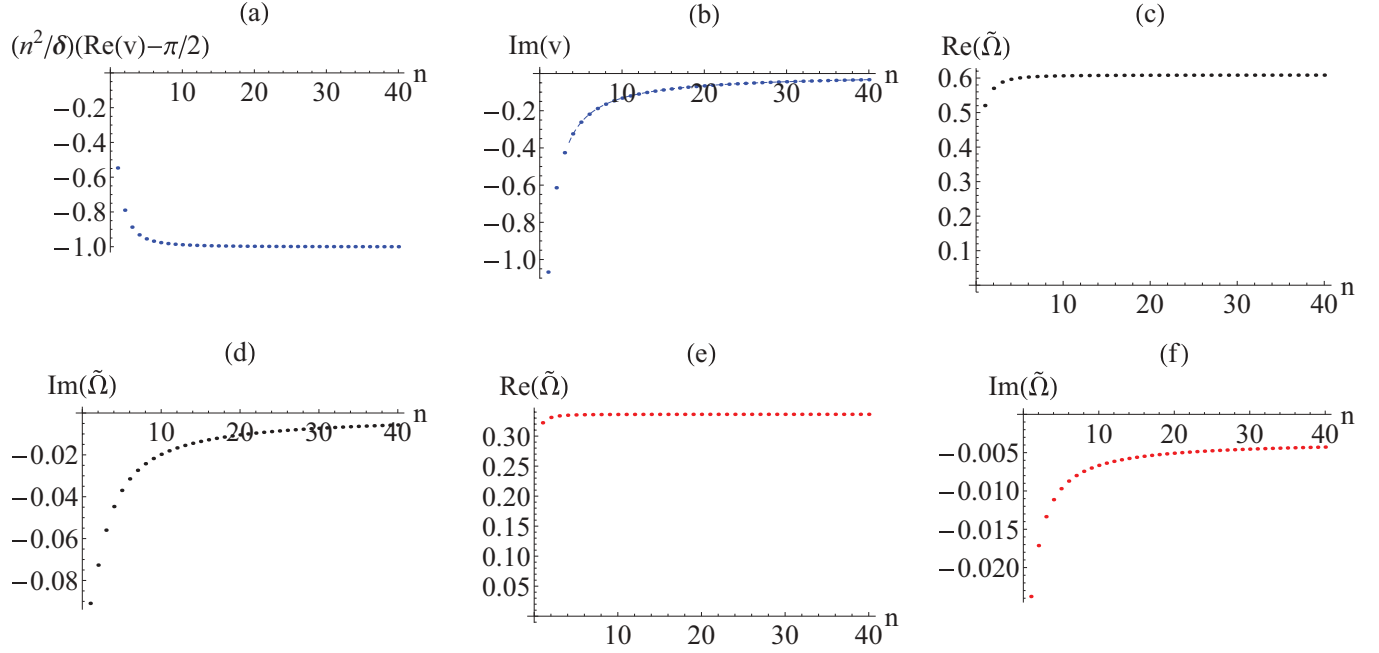


FIG. 6. (Color online) The quantities for the mode with $\text{Re}(v) \cong \pi/2$ are plotted as a function of n , the number of cells. The index of refraction of the dielectric is $n_r = 1.0$. The ratio of the dielectric to metal plate thickness, $\beta = 1$. (a) The deviation of the normalized real part of the wave vector from $\pi/2$. (b) The imaginary part of the normalized wave vector. (c), (d) The normalized real and imaginary parts of the plasmonic resonance frequency with silver as the metal. (e), (f) The normalized real and imaginary parts of the plasmonic resonance frequency with gold as the metal.

The second term on the right-hand side of (36) gives the correction to $\text{Re}(v)$ for large n from $\pi/2$. In Fig. 6(a), I plot the numerically computed value of $(\frac{n^2}{\delta})[\text{Re}(v) - \frac{\pi}{2}]$ as a function of n . The curve goes asymptotically to -1 , as predicted by (36).

The dashed line in Fig. 6(b) plots the approximate asymptotic analytic expression for $\text{Im}(v)$ as deduced from (27) and (36). The agreement with the numerical computation is remarkable for large n .

In Figs. 6(c) and 6(d) and Figs. 6 and 6(f), respectively, the real and imaginary complex eigenfrequencies for both silver and gold are plotted as a function of the number of cells.

Replacing Eq. (36) in Eq. (26), and Taylor expanding in powers of $1/n$, one can obtain approximate analytic expressions for the complex eigenfrequencies of silver and gold for this mode, namely,

$$\begin{aligned} \tilde{\Omega}_{\text{Ag}} \cong & (0.60858 - 0.00096i) + 0.186945 \left(\frac{1}{n}\right) i \\ & - 0.21073 \left(\frac{1}{n}\right)^2 + O\left(\left(\frac{1}{n}\right)^3\right), \end{aligned} \quad (37)$$

$$\begin{aligned} \tilde{\Omega}_{\text{Au}} \cong & (0.336318 - 0.00347i) + 0.0315575 \left(\frac{1}{n}\right) i \\ & - 0.0254728 \left(\frac{1}{n}\right)^2 + O\left(\left(\frac{1}{n}\right)^3\right). \end{aligned} \quad (38)$$

These asymptotic expressions for the resonant frequencies reproduce very accurately the graphs in Figs 6(b), 6(c), 6(d), and 6(f) for $n > 10$.

One notes that the decay rate decreases as n increases, but one needs to go to a much higher value of n than for the mode with $\text{Re}(v) \cong 0$ for the decay rate to be comparable to $\Gamma/2$, thus confirming that the latter mode is the best choice for achieving a narrow resonance.

VII. CONCLUSION

Although the general theory for determining the complex wave numbers of the different modes of an infinite periodic 1D structure has been known for almost 80 years, the particulars of the complex eigenfrequencies for finite number of cells n and for different constituent equations (dispersion relations) need to be computed in detail for different cases.

In this paper, I showed that the mode with $\text{Re}(v) \cong 0$ is the best choice for obtaining narrow plasmonic resonances when the system consists of quarter-wave plates of noble metals alternating with a dielectric. Furthermore, I showed that by varying the ratio of the thicknesses of the dielectric material to that of the metal in each of the unit cells, one can tune the plasmonic frequency, especially for silver, to any desired value in the optical and near-infrared window.

[1] Lord Rayleigh, *Philos. Mag.* **24**, 145 (1887).

[2] N. Brillouin, *Wave Propagation in Periodic Structures* (Dover, New York, 1956).

[3] F. Bloch, *Z. Phys.* **52**, 555 (1928).

[4] See E. C. Titchmarsh, *Eigenfunction Expansion Associated with Second Order Differential Equations* (Oxford University Press, London, 1958).

[5] F. Abeles, *Ann. Phys.* **5**, 596 (1950).

- [6] H. Kogelnik and C. V. Shank, *Appl. Phys. Lett.* **18**, 152 (1971).
- [7] C. V. Shank, J. E. Bjorkholm, and H. Kogelnik, *Appl. Phys. Lett.* **18**, 395 (1971).
- [8] See, for example, J. D. Joannopoulos, S. G. Johnson, J. N. Winn, and R. D. Meade, *Photonics Crystals: Molding the Flow of Light*, 2nd ed. (Princeton University Press, Princeton, NJ, 2008).
- [9] R. Friedberg and J. T. Manassah, *Phys. Lett. A* **372**, 4164 (2008).
- [10] J. T. Manassah, *Phys. Lett. A* **308**, 259 (2008).
- [11] K. L. Kelly, E. Coronado, L. L. Zhao, and G. C. Schatz, *J. Phys. Chem.* **107**, 668 (2003).
- [12] E. Prodan, C. Randloff, N. J. Hallas, and P. Nordlander, *Science* **302**, 419 (2003).
- [13] R. Friedberg and J. T. Manassah, *Chem. Phys. Lett.* **539-540**, 118 (2012).
- [14] S. Mubeen, S. P. Zhang, N. Kim, S. Lee, S. Kramer, H. X. Xu, and M. Moskovits, *Nano Lett.* **12**, 2088 (2012).
- [15] C. Sonnichsen, Dissertation, Ludwig-Maximilians-Universität, Munich, 2001.
- [16] P. B. Johnson and R. W. Christy, *Phys. Rev. B* **6**, 4370 (1972).